Mechanics of Advanced Composite Structures 5 (2018) 149 – 156

Semnan University

Mechanics of Advanced Composite Structures

journal homepage: http://MACS.journals.semnan.ac.ir

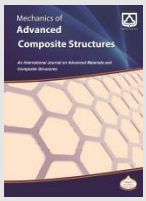

Flexural Behavior of Fiber–Metal Laminates Reinforced with Surface-Functionalized Nanoclay

Sh. Vahedi[a], S.M.H. Siadati[a], H. Khosravi[b*], A. Shahrabi-Farahani[a]

[a] *Materials Science and Engineering Faculty, K.N. Toosi University of Technology, Tehran, Iran*
[b] *Department of Materials Engineering, Faculty of Engineering, University of Sistan and Baluchestan, Zahedan, Iran*

PAPER INFO

Paper history:
Received 2017-12-07
Received in revised form 2018-01-03
Accepted 2018-02-03

Keywords:
Fiber–metal laminates
Nanoclay
Surface functionalization
Three-point bending test
Fracture surface

ABSTRACT

The effects of surface-functionalized Na^+-montmorillonite nanoclay particles on the flexural behavior of E-glass fiber-reinforced aluminum (GLARE) laminates were investigated. The nanoclay particles were subjected to surface functionalization using 3-(trimethoxysilyl)propylamine to increase their compatibility with the epoxy matrix and improve their dispersion within the matrix. Experimental results indicated that the GLARE laminates achieved the highest flexural strength (61%) and energy absorption (51%) at an addition of 3 wt% functionalized nanoclay. The highest flexural modulus (67% increase) was observed at an addition of 5 wt% functionalized nanoclay. The flexural properties of the functionalized nanoclay-filled GLARE laminates were significantly better than those of untreated nanoclay-filled GLARE laminates. Microscopic observations suggested that the introduction of functionalized nanoclay particles markedly enhanced the interfacial adhesion between the matrix and the E-glass fibers.

1. Introduction

Among the various types of composite structures, fiber–metal laminates (FMLs), such as glass fiber-reinforced aluminum (GLARE) laminates, possess high specific strength, outstanding damage tolerance against impact loads, high corrosion resistance, and excellent fatigue properties. They owe such superb qualities to the combined and synergistic properties of fibrous composites and metal alloys [1–5]. FMLs are a new generation of hybrid materials consisting of fiber-reinforced composite layers sandwiched and bonded between two thin metallic plates [6, 7]. These laminates have found applications in various industries, such as the aircraft, marine, civil, and automobile sectors, given their outstanding characteristics.

In 1978, researchers of the National Aerospace Laboratory and Delft University implemented initiatives designed to increase the fatigue life of Al alloys. Their results illustrated that when the alloys are fabricated in the form of laminates and integrated into a thick sheet, the rate of crack growth decreases. Under these conditions, crack nucleation in one layer causes the nucleation to diverge between adhered layers [8, 9]. These initiatives paved the way for substantial developments with regard to fiber stacking sequence, metal surface treatment, and process parameter control, among other areas. Rajkumar et al. [10] showed that the flexural strength of FMLs decreases with increasing strain rate, and Najafi et al. [11] found that the flexural properties of FMLs are affected by hygrothermal aging. Yeh et al. [12] investigated the mechanical properties of hybrid boron/S2-glass/Al FMLs and reported that the highest mechanical response occurs in specimens containing hybrid boron and glass fibers. Dhaliwal et al. [13] examined the flexural properties of Al/carbon fiber–epoxy FMLs. The authors indicated that when composite layers are stacked exterior to

* Corresponding author. Tel.: +98- 054331132642
E-mail address: hkhosravi@eng.usb.ac.ir
DOI: 10.22075/MACS.2018.13315.1130

Al layers, a high flexural modulus and a small strain to failure are attained. Sadighi et al. [14] carried out research on the tensile and flexural properties of GLARE and uncovered that unidirectional glass fiber considerably enhances the mechanical properties of GLARE structures.

Further improvements in the mechanical properties of fibrous composites through the introduction of nanofillers have been reported [15–17]. The introduction of nanofillers is possible through their dispersion into a matrix [18] or their growth on the surface of fibers [19]. Among the range of nanometric fillers available, nanoclay particles are of interest as reinforcement for polymers because of their high reactivity, high surface-to-volume ratio, easy availability, and low cost [20–22]. Montmorillonite (MMT), as a type of clay mineral, has also exhibited considerable potential as a material for fabricating polymer nanocomposites [23, 24]. Nanoclay addition into a polymer matrix enhances many of the polymer's properties, especially its mechanical attributes [20–24]. Accordingly, several works have been devoted to the development of techniques for the homogeneous dispersion of nanoclay in polymer matrices and the improvement of interfacial interaction between nanoclay and matrices [25, 26]. Such enhancements are realized via the functionalization of nanoclay particles [24]. Chan et al. [27] studied the reinforcement mechanism of nanoclay in epoxy matrix nanocomposites by focusing on nanoclay–epoxy interaction. They found that the addition of 5 wt% nanoclay increases tensile strength and modulus by 25% and 34%, respectively. Park et al. [24] reported that the mechanical interfacial properties, critical stress intensity factor (K_{IC}), and interlaminar shear stress of silane-functionalized MMT/epoxy composites are greater than those of untreated ones.

Researchers have also probed into the fabrication of multiscale composites using nanoclay-enhanced matrices in fibrous composites. Chowdhury et al. [28], for instance, investigated the effects of nanoclay on the flexural properties of woven carbon fiber/epoxy composites prepared via vacuum resin transfer molding. The authors demonstrated that an addition of 2 wt% nanoclay enhances the flexural strength and modulus of the composites by 14% and 9%, respectively. However, increasing the nanoclay concentration to 3 wt% diminishes flexural properties because of the agglomeration of nanoclay. Ngo et al. [29] reported that the highest improvements in the tensile properties of glass fiber/epoxy composites are obtained at a concentration of 5 wt% nanoclay. Specifically, the tensile strength and modulus of the composites increase by 10% and 5%, respectively. Karripal et al. [30] found that the flexural properties of glass fiber/epoxy composites improve with nanoclay additions of up to 5 wt% but decline in quality at higher concentrations. Khosravi et al. [31] reported that the tensile, flexural, and compressive strengths of unidirectional basalt fiber/epoxy composites improve by 11%, 28%, and 35%, respectively, after the addition of 5 wt% silane-modified MMT nanoclay in the matrix.

As can be seen, the majority of research on FMLs focused on the design aspects of these structures. The lack of scientific information regarding the effects of nanoparticles on FMLs was the driving force of the present study. This work accordingly evaluated the effects of incorporating different concentrations of functionalized nanoclay into the epoxy matrix on the microstructural modification and, thus, the flexural behavior of Al2024/epoxy–glass fiber GLARE laminates.

2. Experimental

2.1. Materials

KER-828 epoxy resin with polyamine hardener (KUMHO P&B Chemicals Inc., Korea) was used as the matrix material. According to the manufacturer's recommendation, the adopted resin-to-hardener weight ratio was 10:1. Two-dimensional plain weave E-glass fibers with a surface density of 400 g/m^2 (LINTEX Co., China) were used as the reinforcement materials. Al alloy 2024 with a thickness of 0.5 mm was employed to fabricate FMLs. Na^+-MMT nanoclay particles with a surface area of 250 m^2/g were purchased from Sigma-Aldrich Co., USA. Fig. 1 shows the SEM image of the as-received MMT nanoclay powder.

A silane coupling agent known as 3-(trimethoxysilyl) propylamine (3-TMSPA) (Fig. 2) (Merck Chemical Co., Germany) was used for the surface functionalization of nanoclay particles.

Figure 1. SEM image of the as-received MMT nanoclay powder.

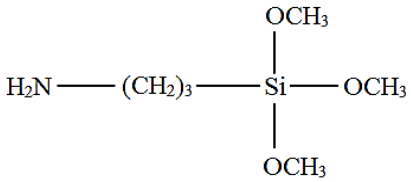

Figure 2. Chemical structure of 3-TMSPA.

2.2. Surface functionalization of nanoclay

For the surface functionalization of nanoclay particles, 5 g of nanoclay was added to a 100 ml solution containing 95% (v/v) ethanol and 5% (v/v) distilled water. Then, 5 g of 3-TMSPA was added to the mixture. Subsequently, ultrasonic waves were applied to the mixture for 10 min using a probe sonicator, after which the mixture was refluxed at 80°C for 7 h [18, 31]. The pH value of the mixture was adjusted to about 4.5 using HCL (37%) [31] to increase the extent of SiOH formation. To separate the functionalized powder, the mixture was centrifuged at 4000 rpm for 30 min. The resultant powder was washed with ethanol three times to eliminate the remaining silane agent and dried at 80°C for 12 h. The silanized nanoclay particles in this paper are referred to as 3-TMSPA/nanoclay.

2.3. Fabrication of GLARE specimens

To fabricate the GLARE laminates, an epoxy/nanoclay mixture was first prepared. Defined weight fractions of 3-TMSPA/nanoclay (0, 1, 3, 5 and 7 wt%) were incorporated into the epoxy resin using an overhead mechanical stirrer (Fintech Co., Korea) at 2000 rpm for 20 min. To ensure the appropriate dispersion of the nanoclay into the epoxy resin, ultrasonic waves were applied to the mixture using a probe sonicator (FAPAN Co., Ltd., Iran) at 120 W for 60 min. Finally, the nanoclay/epoxy mixture was degasified, and a stoichiometric amount of the amine hardener was added. The mixture was manually stirred for 5 min. The surfaces of the Al alloy 2024 sheets were washed with acetone and then scrubbed with a coarse brush. Finally, the Al sheets were submerged in boiling water and again washed with acetone.

The GLARE specimens were fabricated via the hand lay-up method. Four layers of woven E-glass fibers were impregnated with the nanoclay/epoxy mixture and placed between two Al sheets. For the appropriate adhesion of the Al sheets to the fibrous composite layers, the prepared laminates were held in cold static pressing for the entire duration of curing. The stages of GLARE specimen fabrication are shown in Fig 3. For comparison, an FML specimen without nanoclay and another incorporated with 3 wt% untreated nanoclay were also fabricated.

2.4. Three-point bending test

A three-point bending test was performed at room temperature, in accordance with ASTM D790-10. A universal testing machine (Hounsfield H25KS, England) with a capacity of 2.5 ton was used. The cross-head speed was 4.3 mm/min, and the support span-to-thickness ratio was 32:1. Three GLARE specimens were tested, and mean values were obtained.

2.5. Characterization

To identify the functional groups on the surfaces of both the untreated nanoclay and 3-TMSPA/nanoclay particles, Fourier transform infrared (FTIR) analysis was performed using an FTIR-460 Plus (JASCO, Japan). The powders were tested at a wavenumber range of 400 to 4000 cm^{-1} with a resolution of 4 cm^{-1}. The fracture surfaces (in the tensile region under the neutral line) of the specimens subjected to the three-point bending test were examined using field emission scanning electron microscopy (FESEM) (HITACHI S-4160, Japan).

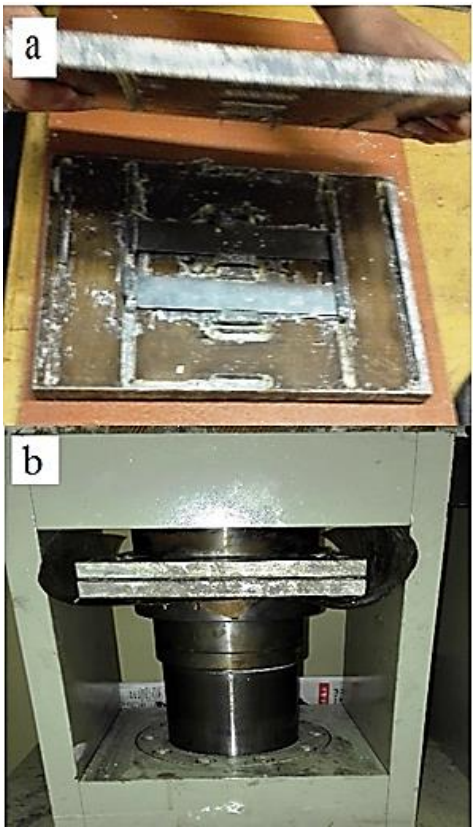

Figure 3. Stages of GLARE specimen fabrication: (a) Hand lay-up and (b) cold static pressing.

3. Results and discussion

3.1. FTIR results

The FTIR spectra of the untreated nanoclay and 3-TMSPA/nanoclay particles are shown in Fig. 4. For the untreated nanoclay particles (Fig. 4a), the peak at 3445 cm^{-1} occurred because of the stretching vibration of hydroxyl (-OH) groups on the surface of the nanoclay, and the peak at 1645 cm^{-1} was caused by the bending vibration of H-O-H [32]. The absorption peak at 3634 cm^{-1} was due to the stretching vibration of the OH groups bonded to the Al atoms, and the peak at 1055 cm^{-1} reflects the stretching vibration of Si-O-Si and Si-O [31]. The absorption bands at 525 and 473 cm^{-1} are related to the bending vibration of Si-O-Si and Si-O-Al groups [33]. The characteristic peak at 805 cm^{-1} stemmed from the symmetric stretching of the Si-O-Si group [31]. The FTIR spectra of the 3-TMSPA/nanoclay (Fig. 4b) show additional bands at 1510 cm^{-1} (N-H bend), 3368 cm^{-1}, and 3292 cm^{-1} (stretching vibrations of NH_2 group) and at 2926 and 2868 cm^{-1} (CH_3 asymmetric stretching and CH_2 stretching), which were caused by the silanization of the nanoclay particles [34–36]. The formation of these bands demonstrated the successful grafting of 3-TMSPA onto the nanoclay particles.

3.2. Results of the three-point bending test

All the specimens tested displayed nearly the same typical behavior (Fig. 5). As evident in the flexural stress–strain curve (Fig. 5a), stress suddenly dropped after it reached its peak value owing to fiber breakage; this decrease was followed by a rise and fall as well as considerable straining due to Al tearing and delamination. Fig. 5b depicts the actual specimen and Al tearing and delamination. For improved comparison and evaluation, the flexural strength, flexural modulus, and energy absorption of all the surface-functionalized specimens were extracted from the flexural stress–strain curves (Fig. 6).

Fig. 6a shows the values and variations in the flexural strength of the specimens at various 3-TMSPA/nanoclay loadings. The specimen containing 3 wt% nanoclay exhibited the highest flexural strength—a 61% improvement. This enhancement in flexural strength is attributed to the strong matrix as well as the improved interfacial bonding between the matrix and the E-glass fibers. Reinforcement with the nanoparticles enabled the matrix to withstand a large degree of applied load and reduced the stress concentration that had to be endured by the fibers [18, 31]. In other words, the friction between the matrix and the glass fibers increased in the presence of the nanoclay particles.

Moreover, the silane coupling agent on the surface of the nanoclay particles drove the formation of a covalent bond between the matrix and the nanoclay, resulting in the elevated performance of the nanoparticles in improving the mechanical properties of the GLARE laminates [24, 25]. Higher quantities of 3-TMSPA/nanoclay in the matrix (i.e., 5 and 7 wt%) reduced the quality of the flexural properties given the agglomeration of nanoparticles in the matrix.

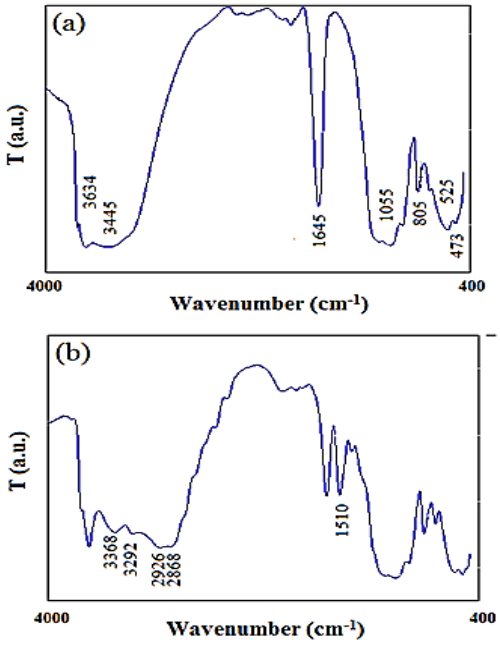

Figure 4. FTIR spectra: (a) Untreated nanoclay and (b) 3-TMSPA/nanoclay particles.

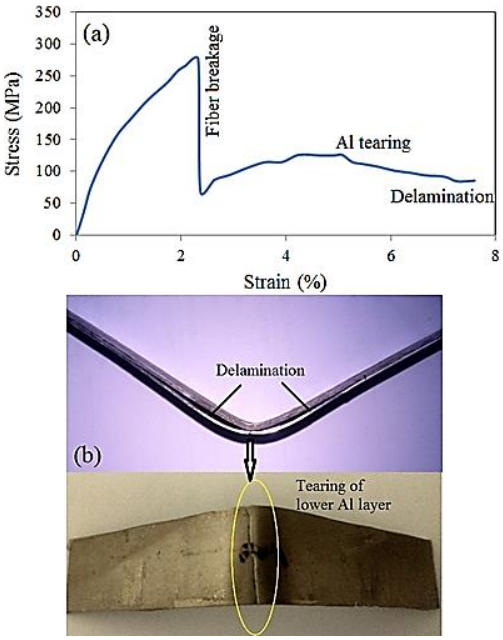

Figure 5. Three-point bending test: (a) Typical flexural stress–strain curve of specimens and (b) failure modes.

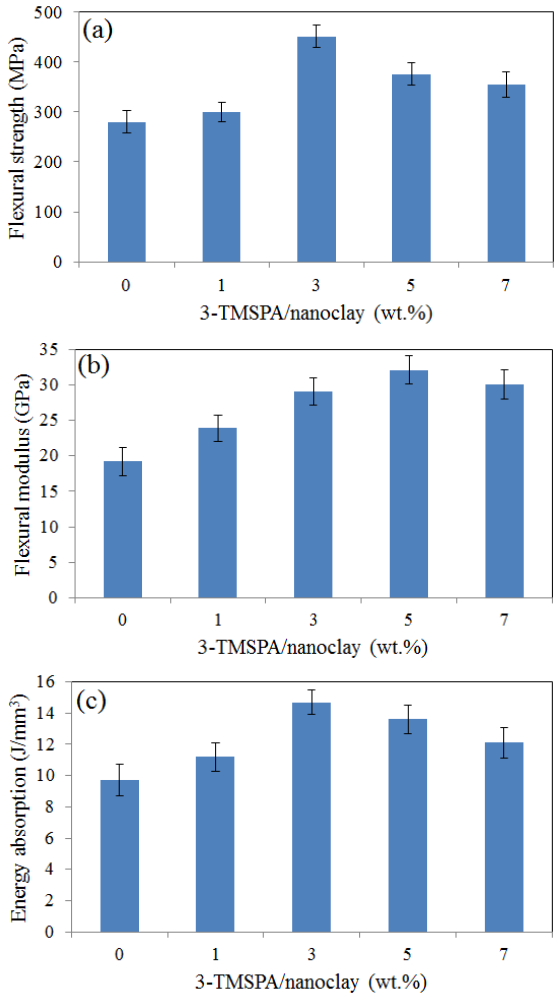

Figure 6. Values and variations in (a) flexural strength, (b) flexural modulus, and (c) energy absorption.

The effects of 3-TMSPA/nanoclay on the flexural modulus of GLARE are displayed in Fig. 6b. The flexural modulus of the specimen containing 5 wt% 3-TMSPA/nanoclay rose to 32.1 GPa, which is equivalent to a 67% increase over the flexural modulus of neat GLARE (19.2 GPa). This result seemed reasonable considering that the ceramic nanoparticles had a higher stiffness than did neat epoxy. Another reason is the fact that the nanoclay particles hindered the movement of polymer chains under loading. Note that the flexural modulus of the specimen containing 7 wt% 3-TMSPA/nanoclay was lower than that of the sample containing 5 wt% 3-TMSPA/nanoclay. Again, this phenomenon is ascribed to the agglomeration of nanoparticles in the matrix, which resulted in weak interaction between the matrix and the nanoparticles.

The energy absorption of the GLARE specimens with different 3-TMSPA/nanoclay concentrations are presented in Fig. 6c. Energy absorption was determined by integrating the total area under the flexural stress–strain curves. The energy absorption of the specimens exhibited the same trend as that of flexural strength. The results also indicated that the maximum energy absorption (i.e., a 51% increase) was achieved with 3 wt% 3-TMSPA/nanoclay. A possible explanation for this behavior is the crack deflection imposed by the nanoclay particles within the matrix [37]. Furthermore, as mentioned previously, the addition of nanoclay particles enhanced the interfacial interaction between the fibers and the matrix. On the other hand, the agglomeration of nanoclay particles in the case of GLARE incorporated with higher concentrations of nanoclay generated stress concentration regions, which were weak points that facilitated crack initiation and growth, finally resulting in decreased energy absorption.

Table 1 presents the results on the effects of surface functionalization on the flexural properties of two GLARE laminates that both contain 3 wt% nanoclay, one containing untreated nanoclay, and another that was treated with silane. The specimen comprising untreated nanoclay showed 19%, 20%, and 17% improvement in flexural strength, flexural modulus, and energy absorption, respectively, whereas the 3-TMSPA/nanoclay specimen showed 61%, 51%, and 51% improvement in the aforementioned properties, respectively. The stronger reinforcement effect in the 3-TMSPA/nanoclay specimen can be credited to the fine dispersion and excellent matrix–nanoclay interaction due to the silanization of the nanoparticles. The superb matrix–nanoclay interaction was assumed to be due to the introduction of TMSPA/nanoclay into the matrix; the amino groups on the surface of the nanoparticles reacted with the epoxide groups of the epoxy matrix, and covalent bonds were created, leading to the outstanding interaction.

Table 1. Flexural properties of GLARE reinforced with untreated and treated nanoclay particles (3 wt%)

Specimen	Flexural modulus (GPa) Improvement (%)	Flexural strength (MPa) Improvement (%)	Energy absorption (J/mm³) Improvement (%)
GLARE	19.2	280	9.72
Untreated nanoclay-filled GLARE	23.1 61%	335 51%	11.4 51%
Treated nanoclay-filled GLARE	29.1 19%	451 20%	14.7 17%

3.3. Microscopic analysis of fracture surfaces

FESEM images of the fracture surfaces of the neat and 3 wt%-filled nanoclay (treated and untreated) specimens are shown in Fig. 7.

The surfaces of the glass fibers in the neat specimen (Fig. 7a) were clean and smooth, indicating weak interfacial bonding between the fibers and the matrix. Conversely, the surfaces of the fibers in the specimen containing 3 wt% untreated or treated nanoclay (Figs. 7b and 7c) were rough, and some parts of the nanocomposite matrix adhered to the fibers, indicating strong interfacial bonding. Thus, fiber–matrix debonding and matrix cracking were the predominant mechanisms in the neat and nanoclay-filled specimens, respectively [38, 39]. As depicted in Fig. 8, at a high loading of 3-TMSPA/nanoclay (i.e., 7 wt%), the main problem was the agglomeration of the nanoclay particles within the matrix, which led to the creation of stress concentration regions and therefore degraded flexural properties.

4. Conclusions

This study inquired into the effects of 3-TMSPA/nanoclay on the mechanical performance of GLARE laminates under transverse loading. For this purpose, GLARE specimens containing various concentrations of 3-TMSPA/nanoclay (1, 3, 5 and 7 wt%) were fabricated. The results drawn are summarized below.

1. The FTIR analysis revealed that the surface functionalization of the nanoclay particles was successfully achieved.

2. The GLARE laminate containing 3 wt% 3-TMSPA/nanoclay showed the highest flexural strength and energy absorption. Compared with the flexural strength and energy absorption of the neat specimen, those of the 3 wt% 3-TMSPA/nanoclay specimen improved by 61% and 51%, respectively.

3. The specimen containing 5 wt% 3-TMSPA/nanoclay showed the highest flexural modulus, which was a 67% increase over the level achieved by the neat specimen.

4. The flexural properties of the GLARE filled with 3-TMSPA/nanoclay were superior to those of the untreated nanoclay-filled GLARE.

5. The FESEM examination of the fracture surfaces indicated that the interfacial adhesion between the glass fibers and the epoxy matrix improved through the addition of the nanoclay particles.

6. The results of this investigation suggested that the addition of 3-TMSPA/nanoclay as a reinforcement material (second reinforcement) is an effective way of enhancing the flexural properties of GLARE laminates.

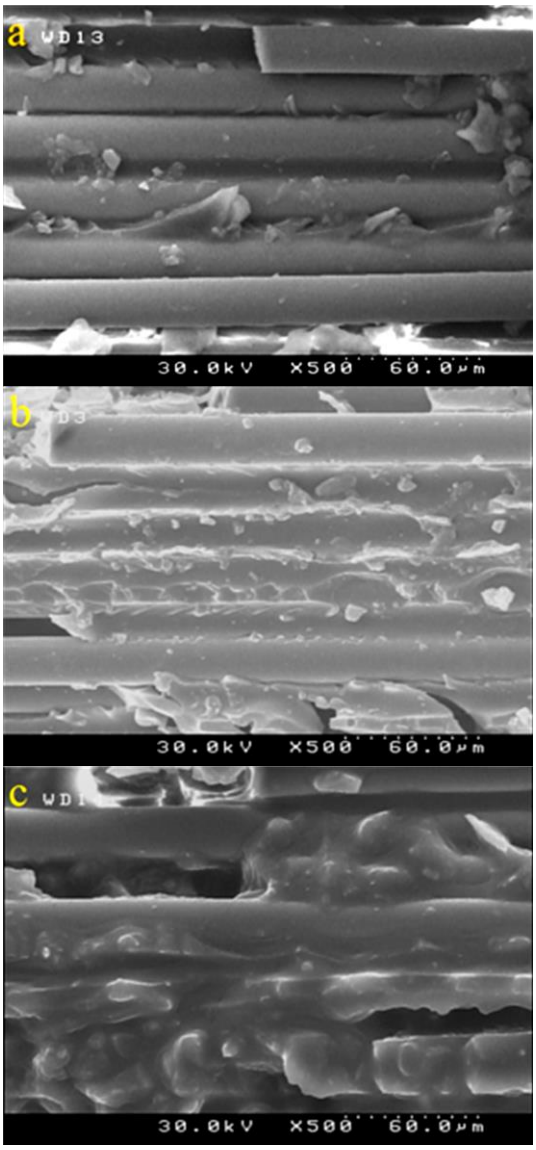

Figure 7. FESEM images of fracture surfaces: (a) Neat specimen, (b) 3 wt% untreated nanoclay-filled specimen, and (c) 3 wt% 3-TMSPA/nanoclay-filled specimen.

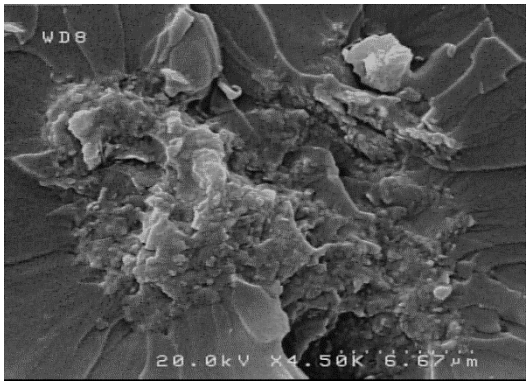

Figure 8. Agglomeration of nanoclay particles on the fracture surface of the specimen filled with 7 wt% 3-TMSPA/nanoclay.

References

[1] Botelho EC, Silva RA, Pardini LC, Rezende MC. A review on the development and properties of continuous fiber/epoxy/aluminum hybrid composites for aircraft structures. *Materials Research* 2006; 9(3): 247-256.

[2] Wu G, Yang JM. The mechanical behavior of GLARE laminates for aircraft structures. *J of the Minerals Metals & Materials Society (JOM)* 2005; 57(1): 72-79.

[3] Dhaliwal GS, Newaz GM. Experimental and numerical investigation of flexural behavior of carbon fiber reinforced aluminum laminates. *J of Reinforced Plastics and Composites* 2016; 35: 945-956.

[4] Chai GB, Manikandan P. Low velocity impact response of fiber-metal laminates-A review. *Composite Structures* 2014; 107: 363-381.

[5] Gonzalez-Canche NG, Flores-Johnson EA, Carrillo JG, Mechanical characterization of fiber metal laminate based on aramid fiber reinforced polypropylene. *Composite Structures* 2017; 172: 259-266.

[6] Prabhakaran RTD, Andersen TL, Bech JI, Lilholt H. Investigation of mechanical properties of unidirectional steel fiber/polyester composites: Experiments and micromechanical predictions. *Polymer Composites* 2016; 37(2): 627-644.

[7] Khalili SMR, Daghigh V, Eslami-Farsani R. Mechanical behavior of basalt fiber reinforced and basalt-fiber metal laminate composites under tensile and bending loads. *J of Reinforced Plastics and Composites* 2011; 30(8): 647-659.

[8] Vermeeren CAJR. An historic overview of the development of fiber metal laminates. Applied *Composite Materials* 2003; 10: 189-205.

[9] Sinmazcelik T, Avci E, Bora OM, Coban O. A review: Fiber metal laminates, background, bonding types and applied test methods. *Materials and Design* 2011; 32: 3671-3685.

[10] Rajkumar GR, Krishna M, Narasimhamurthy HN, Keshavamurthy YC, Nataraj JR. Investigation of Tensile and Bending Behavior of Aluminum based Hybrid Fiber Metal Laminates. *Procedia Materials Science* 2014; 5: 60-68.

[11] Najafi M, Ansari R, Darvizeh A. Environmental Effects on Mechanical Properties of Glass/Epoxy and Fiber Metal Laminates, Part I: Hygrothermal Aging. *Mechanics of Advanced Composite Structures* 2017; 4(3): 187-196.

[12] Yeh PC, Chang PY, Yang JM, Wu PH, Liu MC. Blunt notch strength of hybrid boron/glass/aluminum fiber metal laminates. *Materials Science and Engineering A* 2011; 528: 2164-2173.

[13] Dhaliwal GS, Newaz GM. Experimental and numerical investigation of flexural behavior of carbon fiber reinforced aluminum laminates. *J of Reinforced Plastics and Composites* 2016; 35(12): 945-956.

[14] Sadighi M, Dariushi S. An experimental study of the fiber orientation and laminate sequencing effects on mechanical properties of Glare. *Proc IMechE, Part G: J Aerospace Engineering* 2008; 222: 1015-1024.

[15] Rao PS, Renji K, Bhat MR, Mahapatra DR, Naik GN. Mechanical properties of CNT-Bisphenol E cyanate ester-based CFRP nanocomposite developed through VARTM process. *J of Reinforced Plastics and Composites* 2015; 34(12): 1000-1014.

[16] Zhou Y, Jeelani S, Lacy T. Experimental study on the mechanical behavior of carbon/epoxy composites with a carbon nanofiber-modified matrix. *J of Composite Materials* 2014; 28(14): 3659-3672.

[17] Eslami-Farsani R, Shahrabi-Farahani A. Improvement of high-velocity impact properties of anisogrid stiffened composites by multi-walled carbon nanotubes. *Fibers and Polymers* 2017; 18(5): 965-970.

[18] Khosravi H, Eslami-Farsani R. On the mechanical characterizations of unidirectional basalt fiber/epoxy laminated composites with 3-glycidoxypropyltrimethoxy silane functionalized multi-walled carbon nanotubes-enhanced matrix. *J of Reinforced Plastics and Composites* 2016; 35(5): 421-434.

[19] Du SS, Li F, Xiao HM, Li YQ, Hu N, Fu SY. Tensile and flexural properties of graphene oxide coated-short glass fiber reinforced polyethersulfone composites. *Composites Part B* 2016; 99: 407-415.

[20] Karippa JJ, Narasimha Murthy HN, Rai KS, Sreejith M, Krishna M. Study of mechanical properties of epoxy/glass/nanoclay hybrid composites. *J of Composite Materials* 2011; 45(18): 1893-1899.

[21] Sharma SK, Nema AK, Nayak SK. Effect of modified clay on mechanical and morphological properties of ethyleneoctane copolymer-polypropylene nanocomposites. *J of Composite Materials* 2012; 46(10): 1139-1150.

[22] Hedayatnasab Z, Eslami-Farsani R, Khalili SMR, Soleimani N. Mechanical characterization of clay reinforced polypropylene nanocomposites at high temperature. *Fibers and Polymers* 2013; 14(10): 1650-1656.

[23] Yin X, Hu G. Effects of organic montmorillonite with different interlayer spacing on mechanical properties, crystallization and morphology of

polyamide 1010/nanometer calcium carbonate nanocomposites. *Fibers and Polymers* 2015; 16(1): 120-128.

[24] Park SJ, Kim BJ, Seo DI, Rhee KY, Lyu YY. Effects of a silane treatment on the mechanical interfacial properties of montmorillonite/epoxy nanocomposites. *Materials Science and Engineering A* 2009; 526: 74-78.

[25] Jagtap SB, Rao VS, Ratna D. Preparation of flexible epoxy/clay nanocomposites: effect of preparation method, clay modifier and matrix ductility. *J of Reinforced Plastics and Composites* 2013; 32(3): 183-196.

[26] Ha SR, Rhee KY, Kim HC, Kim JT. Fracture performance of clay/epoxy nanocomposites with clay surface-modified using 3-aminopropyltriethoxysilane. *Colloids and Surfaces A: Physicochemical and Engineering Aspects* 2008; 313-314: 112-115.

[27] Chan ML, Lau KT, Wong TT, Ho MP, Hui D. Mechanism of reinforcement in NCPs/polymer composite. *Composites Part B* 2011; 42: 1708-1712.

[28] Chowdhury FH, Hosur MV, Jeelani S. Studies on the flexural and thermo mechanical properties of woven carbon/NCPs-epoxy laminates. *Materials Science and Engineering A* 2006; 421: 298-306.

[29] Ngo TD, Nguyen QT, Nguyen PT, et al. Effect of NCPs on thermo mechanical properties of epoxy/glass fiber composites. *Arabian J for Science and Engineering* 2016; 41: 1251-1261.

[30] Karripal JJ, Murthy HNN, Rai KS, Sreejith M, Krishna M. Study of mechanical properties of epoxy/glass/NCPs hybrid composites. *J of Composite Materials* 2011; 46(18): 1893-1899.

[31] Khosravi H, Eslami-Farsani R. Enhanced mechanical properties of unidirectional basalt fiber/epoxy composites using silane-modified Na+-montmorillonite nanoclay. *Polymer Testing* 2016; 55: 135-142.

[32] Romanzini D, Piroli V, Frache A, Zattera AJ, Amico SC. Sodium montmorillonite modified with methacryloxy and vinylsilanes: influence of silylation on the morphology of clay/unsaturated polyester nanocomposites. *Applied Clay Science* 2015; 114: 550-557.

[33] Mishra AK, Allauddin S, Narayan R, Aminabhavi TM, Raju KVSN. Characterization of surface-modified montmorillonite nanocomposites. *Ceramic International* 2012; 38: 929-934.

[34] Bertuoli PT, Piazza D, Scienza LC, Zattera AJ. Preparation and characterization of montmorillonite modified with 3-aminopropyltriethoxysilane. *Applied Clay Science* 2014; 87: 46-51.

[35] Shanmugharaj AM, Rhee KY, Ryu SH. Influence of dispersing medium on grafting of aminopropyltriethoxysilane in swelling clay materials. *Journal of Colloid and Interface Science* 2006; 298: 854-859.

[36] Huskic M, Zigon M, Ivankovic M. Comparison of the properties of clay polymer nanocomposites prepared by montmorillonite modified by silane and by quaternary ammonium salts. *Applied Clay Science* 2013; 85: 109-115.

[37] Khan SU, Iqbal K, Arshad Munir, Kim JK. Quasi-static and impact fracture behaviors of CFRPs with nanoclay-filled epoxy matrix. *Composites Part A* 2011; 42: 253-264.

[38] Eslami-Farsani R, Khalili SMR, Hedayatnasab Z, Soleimani N. Influence of thermal conditions on the tensile properties of basalt fiber reinforced polypropylene-clay nanocomposites. *Materials and Design* 2014; 53: 540-549.

[39] Khosravi H, Eslami-Farsani R. On the flexural properties of multiscale nanosilica/E-glass/epoxy anisogrid-stiffened composite panels. *Journal of Computational and Applied Research in Mechanical Engineering* 2016; 7: 99-108.